EVALUATION OF FAILURE MECHANISM OF 3D SPATIALLY VARIABLE SLOPE USING CONDITIONAL SIMULATION

Tokyo Institute of Technology Student Member ○Lihang Hu
Tokyo Institute of Technology Regular Member Akihiro Takahashi

1. INTRODUCTION

It is known that the spatial viability of soil properties affects slope stability. To reveal the spatially varied soil properties in the ground, the Cone Penetration Test (CPT) is commonly used, but a very large amount of CPT data is needed for an accurate estimation. This paper firstly investigates the sampling efficiency with a limited number of CPT measurements for reconstructing the spatially varied soil properties in the 3D slope, then identifies the failure mechanisms and evaluates its relationship with stability number N_s and sliding volume V considering different sampling locations. The soil cohesion c and friction angle tan ϕ are treated as random fields, and Limit Equilibrium Method (simplified Bishop) is used to evaluate the responses of slope stability. The conditional simulation with the Monte-Carlo simulation (MCS) is performed to evaluate the effect of sampling location and the slope failure mechanism.

2. CONDITIONAL RANDOM FIELD

2.1 Conditional simulation

Usually, the spatial variability of shear strength, c and tan ϕ, and soil unit weight γ, are treated as random fields, which can be directly embedded in numerical Limit analysis and Limit Equilibrium Method, namely using the unconditional random fields to evaluate the effect of soil spatial variability on the slope stability [1,2]. However, such unconditional simulations result in an unrealistic range of response in the estimation of slope stability due to no mention of making use of the spatial distribution of related measurement data to constrain the random field. The conditional random field remedies this situation as the measurements are preserved [3]:

$$Z_{\mathrm{c}}(x) = Z_{\mathrm{u}}(x) + [Z_{\mathrm{km}}(x) - Z_{\mathrm{ks}}(x)] \qquad (1)$$

where $Z_{\mathrm{c}}(x)$ is a conditional random field, $Z_{\mathrm{u}}(x)$ is an unconditional random field generated by using Fast Fourier transform (FFT), $Z_{\mathrm{km}}(x)$ is Kriged field based on measured values at x_i (i = 1,2,…,n), $Z_{\mathrm{ks}}(x)$ is Kriged field based on unconditionally simulated values at the same location x_i (i = 1,2,…,n) and n is the number of measurements.

2.2 Kriging

Kriging is a geostatistic method, to make estimates in space. It incorporates the variogram for interpolation that is modelled by a Gaussian process governed by prior covariances, and the information on the spatial correlation of the measured points is used to estimate the weight parameter, as shown in the following equation:

$$\hat{Z}(x) = \sum_{i=1}^{n} \lambda_i Z_i \qquad (2)$$

where the $\hat{Z}(x)$ is the Kriging estimation based on the observations of $Z_1, Z_2, \ldots, Z_n$. n denotes the total number of observations and λ_i denotes the unknown weighting parameter associated with the observations Z_i.

3. SIMULATION RESULTS

3.1 Conditional random field

In this study, the unconditional random field is generated using FFT with an exponential Gauss Markov correlation function. The shear strength c and tan ϕ, and are treated as isotropic random fields. The pseudo-CPT measurements are assumed as the measured data, as CPT is commonly used for estimating the spatial variability of soil properties.

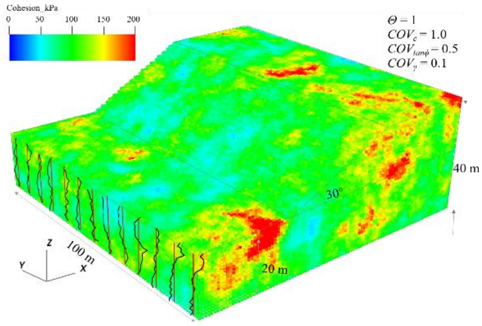

Fig. 1 Model considering the spatial variability of shear strength

Table 1. Input parameters

Parameter	Value
Angle the of slope, β	30°
Mean soil cohesion, μ_c	100 kPa
COV of cohesion, COV_c	1.0
Mean friction angle, $\mu_{\tan\phi}$	0.5774 (μ_ϕ=30°)
COV of friction angle, $COV_{\tan\phi}$	0.5
Mean unit weight, μ_γ	20 kN/m^3
COV of unit weight, COV_γ	0.1
Ratio of the vertical and horizontal correlation length	1 (Isotropic)
Normalized correlation length, $\Theta = \theta_{\ln\tan\phi}/H = \theta_{\ln c}/H = \theta_{\ln\gamma}/H$	1.0
Monte-Carlo iterations	1000

For simplicity, this study focused on a single soil layer with statistically homogeneous shear strength.

Shown in Fig. 1, the pseudo-CPT samplings are planned in a single row in the y-direction with an 8 m interval. A sampling strategy with 10 m intervals in the x-direction is conducted repeatedly to find the best sampling location. Figure 1 demonstrates one realized random field conditioning the CPT measurements for single row sampling pattern at location x = 1 m (loc_x = 1 m), with a normalized correlation length Θ = 1.0 (θ = 20 m), coefficient of variation of shear strength, COV_c and $COV_{\tan\phi}$ = 1.0 and 0.5. It should be noted that for the next conditionings, the statistic input of random fields keeps the same, sampling location changes to loc_x = 10 m, 20 m,…, 100 m, and 1000 number of MCS is considered for each location.

Keywords: 3D spatially varied slope, Slope failure mechanism, Conditional simulation
Contact address: Ookayama 2-12-1, Meguro City, Tokyo 152-8552, Japan

3.2 Sampling efficiency and failure mechanism

The 3D Limit Equilibrium method is used to estimate the stability number N_s and sliding volume V of the 3D spatially varied slope. The N_s, stability number ratio and sliding volume ratio are given as follow:

$$N_{si} = \frac{F_{si} \cdot \mu_\gamma \cdot H}{\mu_c}, \quad R_{N_s} = \frac{N_{si}}{N_{s\_hom}}, \quad R_V = \frac{V_i}{V_{hom}} \qquad (3)$$

where N_{si} is the stability number, F_{si} is the factor of safety of slope, and i refers ith iteration. μ_γ and μ_c are mean unit weight and mean cohesion, respectively. R_{Ns} is the stability number ratio and R_V is the sliding volume ratio, which considers a stability number and sliding volume for homogeneous slope, N_{s_hom} and V_{hom} respectively.

The uncertainty of responses (e.g. stability number and sliding volume) are quantified by a standard deviation, σ_{Ns} and σ_V. Then the sampling efficiency is evaluated as the reduction of uncertainty:

$$\Delta_{N_{si}} = \frac{\sigma_{Nsi\_c}}{\sigma_{Ns\_un}}, \quad \Delta_{Vi} = \frac{\sigma_{Vi\_c}}{\sigma_{V\_un}} \qquad (4)$$

where σ_{Nsi_c} and σ_{Vi_c} is the standard deviation of N_s and V respectively for conditional simulation at conditioning location of CPT loc_x = i m. σ_{Ns_un} and σ_{V_un} is the standard deviation of stability number and sliding volume respectively for unconditional simulation.

Figure 2 plots the variance reduction ratios Δ_{N_s} and Δ_V against sampling locations in the x-direction. The uncertainties in slope stability response are reduced after preserving the measurements in a random field. An optimal sampling location is found at the loc_x = 60 m (near the slope crest) for both N_s and V, that is, the uncertainty is at a minimum value, 30% reduced for N_s and 20% reduced for V when the CPT are sampled at loc_x = 60 m. Comparing the uncertainty reduction for N_s and V, it is suggested that in general, the uncertainty in N_s reduced more than that in V.

Figure 3 reveals the share of the failure mechanisms depending on sampling location. The homogeneous and unconditional refer to a slope with homogeneous strength and unconditional random fields, respectively. The base failure 1 (M_{b1}) is a deterministic failure mechanism for a homogeneous slope. After considering the spatial variability (unconditional case), the failure mechanism shows great diversity (four failure mechanisms appear), and the probability of occurrence of M_{b1} is very small (10%), indicating that local failure mechanisms with smaller sliding volume (e.g. base failure 2, face failures 1 and 2) are induced by spatial variability of soil properties. However, after preserving the pseudo-CPT data as the measurements in a random field, the probability of occurrence of the base failure mechanism 1 M_{b1} increases and reaches the maximum value at the optimal sampling location loc_x = 60 m.

Figure 4 shows the relationship between R_{Ns} and R_V when the sampling location is optimum, i.e., loc_x = 60 m, together with the distinction of failure mechanism. The scatter of V is larger than that of N_s, giving a larger variance of V, which suggests that the uncertainty reduction effect is more significant in N_s. This is attributed to the large variation of sliding volume ratio (from 0.37 to 1.37) in base failure 1 M_{b1}. In contrast to other failure mechanisms, their sliding volumes are comparable, and all are small.

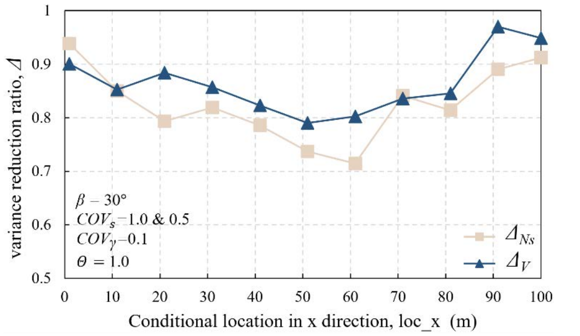

Figure. 2 Δ_{N_s} and Δ_V against conditioning location on the x-direction

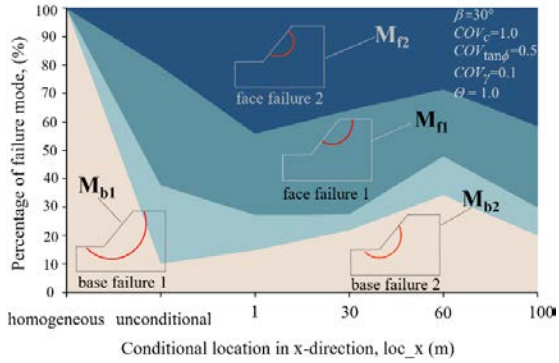

Figure. 3 Percentage of failure mechanism

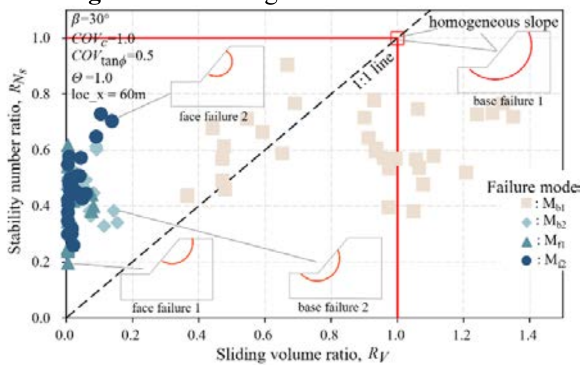

Figure. 4 R_{N_s} against R_V considering failure mechanisms

4. CONCLUSIONS

1) The uncertainty of stability number N_s and sliding volume V are both reduced after conditioning the CPT measurements on the x-axis direction. The optimal sampling location is found at the slope crest (loc_x = 60 m), which reduces 30% and 20% for N_s and V, respectively.
2) The probability of occurrence of the base failure mechanism 1 (M_{b1}) increases after conditioning the CPT measurements. Under the optimal sampling, the sliding volume ratio for the M_{b1} varies largely from 0.37 to 1.37, whereas other failure mechanisms vary from 0.1 to 0.18, small and comparable.

REFERENCES

[1] Kasama K, Whittle A J. Effect of spatial variability on the slope stability using random field numerical limit analyses. *Georisk: Assessment and Management of Risk for Engineered Systems and Geohazards*, 2015; 10(1):42-54.
[2] Hu L H, Kasama K. The effect of spatial variability on the 3D slope stability evaluation. *Proceedings of The Seventh Asian-Pacific Symposium on Structural Reliability and Its Applications (APSSRA2020)*. Oct 4, 2020, Tokyo, Japan.
[3] Gordon A Fenton, Griffiths V D. Risk assessment in geotechnical engineering. *New Jersey: John Wiley & Sons, 2008.*